Covalent Activation of Retinal Rod cGMP-gated Channels Reveals a Functional Heterogeneity in the Ligand Binding Sites

JEFFREY W. KARPEN and R. LANE BROWN

From the Department of Physiology, University of Colorado School of Medicine, Denver, Colorado 80262

ABSTRACT Ion channels gated by the binding of multiple ligands play a critical role in synaptic transmission and sensory transduction. It has been difficult to resolve the contribution of individual binding events to channel gating because ligands are continuously binding and unbinding at each site. In examining the allosteric mechanism of retinal rod cGMP-gated channels, we have circumvented this problem by making use of a cGMP derivative, 8-*p*-azidophenacylthio-cGMP (APT-cGMP), that can be covalently tethered to the binding sites in the presence of long-wavelength UV light. In excised membrane patches, a population of channels was isolated that contained covalently-attached ligands at all but one site. Activation of these channels by cGMP revealed a previously unknown heterogeneity in the ligand-binding sites. The dose-response relations were much shallower than predicted by single-site activation models, but were well described by models in which there are two populations of sites, in roughly equal proportion, that bind cGMP with apparent affinities that differ by a factor of ~25. The two apparent affinities, incorporated into a four-site model of the channel, provided an accurate description of the patch's original dose-response relation. A comparison of results on native and expressed channels suggests that the heterogeneity in the native channel arises at least in part from the presence of two different cGMP-binding subunits.

INTRODUCTION

A fundamental question in the study of ion channels is how individual protein subunits or domains participate in the process of gating. A variety of ion channels are gated or opened by the binding of multiple ligands, each associating with a separate subunit or domain (reviewed in Andersen and Koeppe, 1992; Barnard, 1992; Unwin, 1993; Catterall, 1994). The ligands for this group of channels include neurotransmitters and intracellular messengers such as Ca^{2+}, cyclic nucleotides, and phosphoinositides. It has been difficult to assess the contribution of each binding step to gating because methods have not been available to study each event in isolation. Covalent tethering of one or more ligands to a channel allows the functional consequences of ligand binding to the remaining sites to be measured without the complications of the original (tethered) ligands dissociating and rebinding. This approach provides information on individual binding-site behavior that cannot be extracted from a conventional analysis of dose-response relations using free ligand alone.

Address correspondence to Dr. Jeffrey W. Karpen, Department of Physiology, C240, University of Colorado School of Medicine, 4200 East Ninth Avenue, Denver, CO 80262.

Dr. Brown's present address is R.S. Dow Neurological Sciences Institute, 1120 NW 20th Avenue, Portland, Oregon 97209.

Channels directly gated by the binding of cyclic nucleotides are emerging as a key component of signaling systems in a variety of cell types (reviewed in Yau, 1994; Zimmerman, 1995; Kaupp, 1995). This type of channel was first discovered in retinal rods (Fesenko et al., 1985), where it is known to generate a membrane hyperpolarization in response to the light-triggered hydrolysis of cGMP (reviewed in Yau and Baylor, 1989; Stryer, 1991; Pugh and Lamb, 1993; Yarfitz and Hurley, 1994). When purified from bovine rods, the native channel contains two subunits of 63- and 240-kD molecular mass (Kaupp et al., 1989; Hsu and Molday, 1993; Chen et al., 1993; Chen et al., 1994; Körschen et al., 1995), both of which bind cGMP (Brown, Gerber, and Karpen, 1993*b*; Brown et al., 1995). While significant activation of the channel requires the binding of at least three molecules of cGMP (Haynes et al., 1986; Zimmerman and Baylor, 1986; Karpen et al., 1988*a*), the role of each subunit type in channel activation is not clear.

The rod channel is an ideal candidate for the kind of analysis described above because, unlike the neurotransmitter-gated channels, it does not desensitize upon exposure to its activating ligand (Fesenko et al., 1985; Karpen et al., 1988*b*). In a previous study, exposure of excised membrane patches from salamander rod outer segments to a photoaffinity analogue of

 J. GEN. PHYSIOL. © The Rockefeller University Press • 0022-1295/96/02/169/13 $2.00
Volume 107 February 1996 169–181

cGMP, 8-*p*-azidophenacylthio-cGMP (APT-cGMP), in the presence of 350 nm light was shown to result in a persistent current that could not be removed by extensive perfusion with cGMP-free solution (Brown et al., 1993*b*). This current displayed a number of properties that precisely mimicked the behavior of currents through cGMP-activated channels, indicating that the persistent current arose from irreversibly activated channels in which cGMP moieties were covalently tethered to the ligand-binding sites. This conclusion was also supported by biochemical studies in which APT-[^{32}P]-cGMP was found to specifically label both the 63- and 240-kD subunits of the bovine rod channel (Brown et al., 1993*b*; Brown et al., 1995).

In the current study we have begun to exploit this effect by studying the activation of channels missing only a single ligand. To achieve this condition, >80% of the channels in a patch were covalently activated. Binomial statistics then predicts that channels missing only their last ligand will outnumber those missing two or more ligands by a factor of ~15. Analysis of the dose-response relation for these remaining channels indicated the presence of two distinct populations, present in roughly equal proportions, that were activated by cGMP with apparent affinities that differed by a factor of ~25.

METHODS

Reagents and Preparations

cGMP and 8-Br-cGMP were purchased from Sigma Chemical Co. (St. Louis, MO). APT-cGMP was synthesized as described previously (Brown et al., 1993*b*). Native cGMP-gated channels were studied in excised, inside–out membrane patches from retinal rod outer segments of the leopard frog, *Rana pipiens* (maintained at 4°C as described in Gordon et al., 1992). A few experiments were done for comparison on patches from the larval tiger salamander, *Ambystoma tigrinum* (maintained as described in Baylor and Nunn, 1986). The methods used to obtain isolated cells and outer segments for recording have been described (Brown et al., 1993*a*). Expressed homomultimeric channels were studied in patches excised from *Xenopus* oocytes injected with cRNA coding for the bovine α subunit. The cDNA clone was kindly provided by Dr. William Zagotta (University of Washington School of Medicine, Seattle, WA). The amino acid sequence is identical to the published sequence (Kaupp et al., 1989). RNA was transcribed from the cDNA and injected into *Xenopus* oocytes using previously described methods (Zagotta et al., 1989). Typically, each oocyte was injected with 50 nl of a 1 ng/nl solution of RNA.

Electrophysiology

Patch-clamp experiments on native rod channels were performed as described (Brown et al., 1993*a, b*). For experiments on expressed channels in oocytes, patch electrodes had resistances ≤1 MΩ. In all experiments, the solution in the patch pipette and experimental chamber contained 130 mM NaCl, 2 mM Hepes (pH 7.6), and 0.02 mM EDTA, with cyclic nucleotides added as indicated. Currents were evoked by +50-mV pulses (50 ms in duration) from a holding potential of 0 mV. They were low-pass filtered at 2 kHz and sampled at 10 kHz. To determine the cGMP dose–response relation before covalent activation of channels, leak currents in the absence of cGMP were subtracted. Currents at low cGMP concentrations were measured after a steady state was reached. Currents at high cGMP concentrations were measured within 2 ms of switching the voltage to minimize ion depletion effects (Zimmerman et al., 1988); changes in gating were complete within that time (Karpen et al., 1988*a*). For covalent activation of channels, patches were exposed to APT-cGMP and illuminated with long-wavelength UV light as described (Brown et al., 1993*b*). The output of the 200-W mercury lamp (Spectral Energy, Westwood, NJ) was screened with both a 360-nm bandpass filter (UG 1; Schott Glaswerke, Mainz, Germany) and an IR blocking filter (51950; Oriel Corporation, Stratford, CT). The latter filter prevented warming of the experimental chamber, and further attenuated wavelengths <320 nm. After exposure, patches were washed for 15 min in nucleotide-free solution to remove all untethered cyclic nucleotide (see text). To determine the persistent current through cGMP-gated channels, the leak current was measured by perfusing the patch with 5 mM $MgCl_2$, which blocks 96–98% of the Na^+ current through the channel (Brown et al., 1993*b*). To obtain the dose-response relation for free cGMP atop a level of persistent current, the persistent current was subtracted from total currents in the presence of cGMP. Atop persistent currents that were >70% of the maximum patch current, it was difficult to measure cGMP-induced currents that were less than one-tenth of the remaining current induced by saturating cGMP. There were two reasons for this: the primary reason is that the persistent current under these conditions is much larger than the cGMP-induced current, and small percentage fluctuations in the persistent current due to changes in the leak or changes in the maximum patch current can obscure the cGMP-induced currents. Second, the increase in current after the application of cGMP was often quite small (tens of picoamperes). For these reasons, the changes in current at the lowest cGMP concentrations were usually measured several different times during the patch. Although fits of the Hill equation to dose–response data do depend somewhat on the range of I/I_{max} values, the conclusions are not affected by the smaller range that was fit atop high levels of permanent activation. Prior to covalent activation, Hill coefficients >1.5 were consistently required to fit I/I_{max} values between 0.1 and 1.0.

Graphical Representation of Data and Curve Fitting

The fraction of maximum current vs cGMP concentration is plotted on double-log coordinates throughout this paper. This was done for two reasons. First, in each experiment a several thousand-fold range of cGMP concentrations was tested, which gave rise to currents that often varied over several orders of magnitude. On both linear and semi-log plots, the data at low concentrations would be very compressed. Second, on a double log plot, the slope at low ligand concentrations approaches the minimum number of ligands required to activate the channel (Haynes et al., 1986; Zimmerman and Baylor, 1986). In this study, the average number of ligands that need to bind to cause activation decreases with increasing levels of covalent liganding.

The fits shown are to the log values of the fraction of maximum current. In most cases, the fits to the linear values were very

similar. In those cases in which there is some discrepancy, however, both sets of parameters are included, and more weight is given to the linear fit parameters. In fitting equations to the log values, one assumes that uncertainties are equal on a log scale, which underestimates the uncertainties at small values of the fraction of maximum current. Curve fitting and plotting were done with Sigma Plot 2.0 software for Windows (Jandel Scientific, San Rafael, CA).

Equations for Channel Models

Several mechanisms that can account for the observed heterogeneity in the final binding step are considered in Figs. 5 and 6. As a way of distinguishing between them, we have determined whether they provide a good description of the original dose–response relation of a patch. For each mechanism, the equations relating the apparent dissociation constants at the final binding site to intrinsic dissociation constants and channel closing equilibrium constants are given in the text. The equations that describe the dose-reponse relations for unliganded channels are given below. In each model, O_L represents the fraction of channels in the large conducting state, O_S is the fraction of channels in the small conducting state, and r is the ratio of the open channel conductance of the small state to that of the large state. I/I_{max} is the fraction of the maximum current at saturating cGMP. The other quantities are defined in the text.

Model 1 (Figs. 5 *A* and 6 *A*):

$$O_L = [cGMP]^4/\{[cGMP]^4 + K_L\{[cGMP]^4 + 2[cGMP]^3(K_A + K_B) + [cGMP]^2(K_A^2 + 4K_AK_B + K_B^2) + 2[cGMP](K_A^2K_B + K_AK_B^2) + K_A^2K_B^2\}\}$$

$$I/I_{max} = O_L(1 + K_L).$$

Model 2 (Figs. 5 *B* and 6 *B*):

$$O_L = [cGMP]^4/\{[cGMP]^4 + K_L\{[cGMP]^4 + 2[cGMP]^3(K_A + K_B)(1 + 1/K_S) + [cGMP]^2(K_A^2 + 4K_AK_B + K_B^2) + 2[cGMP](K_A^2K_B + K_AK_B^2) + K_A^2K_B^2\}\}$$

$$O_S = 2O_LK_L(K_A + K_B)/(K_S[cGMP])$$

$$I/I_{max} = (O_L + rO_S)(1 + K_L).$$

Model 3 (Figs. 5 *C* and 6 *C*):

$$O_L = [cGMP]^4/\{[cGMP]^4 + K_L\{[cGMP]^4 + 2[cGMP]^3K_A(2 + 1/K_S) + 6[cGMP]^2K_A^2 + 4[cGMP]K_A^3 + K_A^4\}\}$$

$$O_S = 2O_LK_LK_A/(K_S[cGMP])$$

$$I/I_{max} = (O_L + rO_S)(1 + K_L).$$

Model 4 (Fig. 6 *D*):

$$O_L = 0.5[cGMP]^4/\{[cGMP]^4 + K_L([cGMP] + K_A)^4\} + 0.5[cGMP]^4/\{[cGMP]^4 + K_L([cGMP] + K_B)^4\}$$

$$I/I_{max} = O_L(1 + K_L).$$

RESULTS AND DISCUSSION

Time Course of Covalent Activation

Currents activated by the reversible binding of cGMP or by the covalent tethering of cGMP moieties to channels were studied in excised, inside–out membrane patches. In Fig. 1, persistent currents at +50 mV through cGMP-gated channels are plotted as a function of the time of exposure to APT-cGMP and UV light. The persistent currents are expressed as a fraction of the maximum cGMP-induced current of the patch. One set of data (*closed circles*) was obtained on native channels from a frog rod outer segment, and the other (*open circles*) on expressed homomultimeric channels from a *Xenopus* oocyte that was injected with cRNA coding for the bovine 63-kD (α) subunit (Kaupp et al., 1989). During exposure, the patches were continuously perfused with a nearly saturating concentration of fresh APT-cGMP (10 μM for native channels and 20 μM for expressed channels). This helped to ensure that covalent attachment of ligand occurred randomly, and not with an efficiency based on binding-site affinity. After each time point, patches were washed for 15 min with nucleotide-free solution to ensure that all of the untethered cyclic nucleotide was removed. We have noted that, after photolysis, a small component of the current (typically <10% of the APT-cGMP-induced current) decays on a time scale that is much longer than the time required to perfuse the chamber. Although changing the solution in the entire chamber normally takes only 20–30 s, the slow component often takes 10 min or more to completely decay. Once this component has been removed, however, the remaining "persistent" current is stable for the lifetime of the patch (as long as 8 h). We attribute the slowly-decaying component to photolysis products of APT-cGMP that may partition into the patch membrane or attach to the channel protein via linkages that are relatively labile. The two time courses in Fig. 1 are very similar; the small difference in the kinetics is probably not significant, as partial time-course data from other patches exhibited about this much variation. The close correspondence

between the two time courses suggests that α subunits from different species, as well as the different cGMP-binding subunits within the native channel label with similar efficiency. These time courses were used in subsequent experiments to estimate the exposure times required to achieve a certain level of covalent activation.

Activation of Channels by cGMP Atop Different Levels of Covalent Liganding

Fig. 2 shows cGMP dose-response relations for frog rod channels before covalent activation, and for channels that were not yet fully activated when a persistent current of 15 or 82% of the maximum was obtained. For the latter two relations, I/I_{max} represents the increase in current caused by cGMP normalized by the maximum increase caused by saturating cGMP (85 or 18% of the original maximum current). The purpose of the experiment was to determine the cGMP dose–response relations for channels that already have an average of one or more ligands covalently attached. Two changes are apparent in the relations after covalent activation. A higher percentage of channels were activated at a given cGMP concentration, and the slope of the relations became progressively shallower. Both changes are expected of channels that contain one or more permanently-attached ligands: (*a*) subsaturating concentrations of cGMP should be more effective because the probability that these channels will be fully liganded at any given cGMP concentration is higher. Furthermore, earlier work suggests that cGMP binds cooperatively (Zimmerman and Baylor, 1986); it has been proposed that the last one or two ligands bind with higher apparent affinity because of conformational changes to open states (Karpen et al., 1988*a*; Haynes and Yau, 1990; Taylor and Baylor, 1995). (*b*) Progressively shallower relations are expected because fewer and fewer ligands are required to activate the channels. At low ligand concentrations, the slope of the relation on double-log coordinates approaches the minimum number of ligands necessary to cause measurable activation (Haynes et al., 1986; Zimmerman and Baylor, 1986). In the figure, data from three patches were combined by expressing cGMP concentrations relative to the concentration that gave a half-maximal current before covalent activation (Zimmerman and Baylor, 1986; Brown et al., 1993*a*). When normalized in this way, the corresponding dose-response relations from different patches superimpose. This indicates that the magnitudes of the shifts in the dose–response relations atop different levels of covalent activation were consistent across patches and over a severalfold range of absolute sensitivities to cGMP.

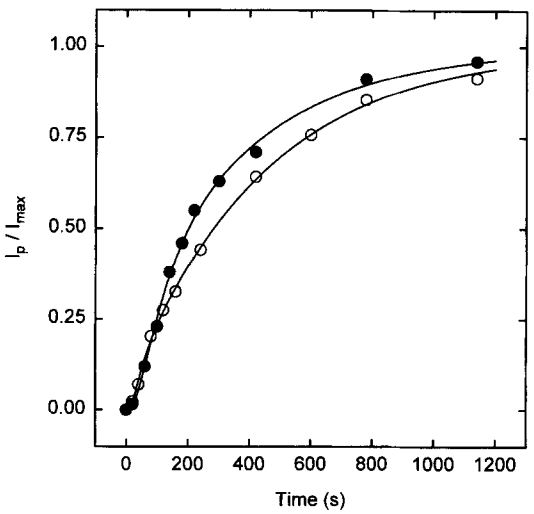

FIGURE 1. Covalent activation of native and expressed cGMP-gated channels as a function of time of exposure to APT-cGMP and UV light. I_p represents persistent current in response to brief +50 mV pulses, after a patch was exposed for the indicated times to APT-cGMP and UV light and then perfused for 15 min with nucleotide-free solution. Concentrations of APT-cGMP are given in the text. I_{max} was the current caused by a saturating concentration of cGMP (1–2 mM) before exposure to APT-cGMP. After exposure, the maximum current was remeasured periodically as the sum of the persistent current and the current induced by saturating cGMP. All currents were leak-subtracted (see Methods). (*Closed symbols*) Data on native channels from a frog rod outer segment; (*open symbols*) data on expressed channels from a *Xenopus* oocyte injected with cRNA coding for the bovine α subunit. I_{max} values were 706 pA (native) and 5,210 pA (expressed). Smooth curves were drawn by eye.

A central goal of this study was to isolate a population of channels in which all but one ligand was covalently attached, and then proceed to measure the resulting dependence of channel activation on free cGMP concentration. In defining the appropriate conditions for this experiment, we initially made three simplifying assumptions. The first was that covalent attachment of cGMP moieties to channel binding sites is a random process. The very similar time-courses for covalent activation of native channels and expressed homomultimers of the α subunit (Fig. 1) argues that this assumption was reasonable. Under these circumstances, the probability that a channel will contain a certain number of covalently attached ligands is given by the binomial distribution:

$$f(x) = \frac{n!}{(n-x)!x!}\, p^x q^{n-x}, \qquad (1)$$

where n is the total number of ligand-binding sites, x is the number of sites to which APT-cGMP is covalently attached, p is the probability that a particular site is labeled, and q is the probability that a particular site is not labeled $(1 - p)$. The second assumption we made was that $n = 4$. Several groups have now reported fits of the Hill equation to dose–response data with coefficients >3 (Kaupp, 1991; Hsu and Molday, 1993; Brown et al., 1993*a*). Furthermore, analysis presented later

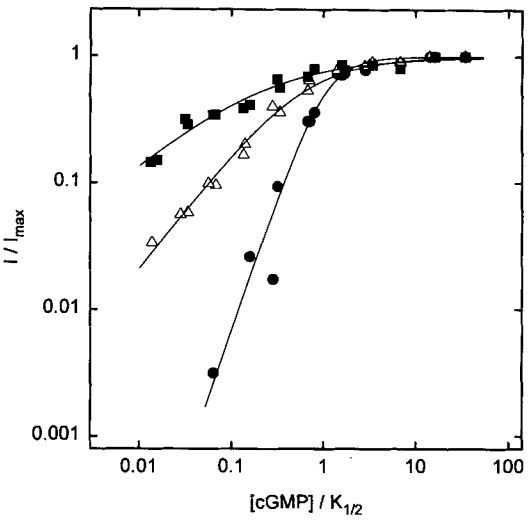

FIGURE 2. Double logarithmic plot of cGMP dose–response relations for rod channels atop different levels of covalent activation. I represents currents activated by free cGMP at +50 mV. I_{max} for each relation is the change in current induced by a saturating concentration of cGMP, and is equivalent to the original maximum current of a patch minus the persistent current. Data from three frog rod patches were combined by expressing cGMP concentrations relative to the concentration that gave a half-maximal current before covalent activation ($K_{1/2}$). (*Closed circles*) Data before exposure to 10 μM APT-cGMP and UV light; (*open triangles*) data atop a persistent current that was, on average, 15% of the original maximum current (12% on one patch and 17% on another); (*closed squares*) data atop a persistent current that was, on average, 82% of the original maximum current (77% on one patch and 87% on another). The original maximum currents and $K_{1/2}$ values for the three patches were: 700 pA and 15.4 μM (0, 12, 77%); 1,280 pA and 36.7 μM (0, 17%); 4,810 pA and 32.7 μM (0, 87%). The smooth curves are fits to the data with a modified form of the Hill equation:

$$I/I_{max} = \frac{([cGMP]/K_{1/2})^n}{([cGMP]/K_{1/2})^n + (K_{1/2\text{-}p}/K_{1/2})^n},$$

in which n is the Hill coefficient (an index of cooperativity), and $K_{1/2\text{-}p}$ is the concentration of cGMP that causes a half-maximal change in current atop the persistent current. The numerator and denominator of the Hill equation were divided by $K_{1/2}$ so that cGMP concentrations could be expressed relative to this value. The fit parameters were as follows: 0% persistent current, n = 2.2 and $K_{1/2\text{-}p}/K_{1/2}$ = 1.0; 15% persistent current, n = 0.97 and $K_{1/2\text{-}p}/K_{1/2}$ = 0.54; 82% persistent current, n = 0.65 and $K_{1/2\text{-}p}/K_{1/2}$ = 0.18.

suggests that dose–response data from the same patch before covalent activation and atop high levels of covalent activation are more easily fit with four-site models of the channel, than with either three-site or five-site models. Finally, in calculating the value of p, we have assumed that the fraction of maximum current is equal to the fraction of fully liganded channels, which implies that channels containing less than the full complement of ligands do not contribute to the current. Under these conditions, $f(4)$ is equivalent to the fractional persistent current (0.15 or 0.82 in the experiments in Fig. 2), and $p = f(4)^{0.25}$ (Eq. 1). Values of $f(x)$ were then calculated for other values of x. At a fractional persistent current of 0.82, the probability that any given site is labeled is 0.95, and the fractions of channels containing 0, 1, 2, and 3 ligands, are predicted to be 5.5×10^{-6}, 4.3×10^{-4}, 0.013, and 0.17. Aside from channels that are fully liganded, the predominant form of the channel is one in which a single ligand is missing. Triply liganded channels are predicted to outnumber channels that are doubly liganded by a factor of ~13. For comparison, at a fractional persistent current of 0.50, triply liganded channels are 3.5 times as abundant as doubly liganded channels, and at a fractional persistent current of 0.15, triply liganded and doubly liganded channels are about equally abundant (with each about three times as abundant as singly liganded channels).

The conclusion that inactive channels are missing only one ligand at a fractional persistent current of 0.82 does not depend on any of the foregoing assumptions. If n = 3 or n = 5, channels missing one ligand are expected to outnumber channels missing two ligands by factors of 15 or 12, respectively. Similarly, one can relax the assumption that only fully liganded channels contribute to the current, and reach the same conclusion. Two conducting states have been observed in native rod channels (Haynes et al., 1986; Zimmerman and Baylor, 1986). In a recent study, the open-channel conductances of the two states were estimated to be 25 and 4 pS (Taylor and Baylor, 1995). The fraction of time in the lower conductance state decreased with increasing cGMP concentration, suggesting that this state may arise from the opening of a partially liganded channel. If one assumes that a channel containing three ligands contributes 16% as much current on average as a channel containing four ligands (a conductance ratio of 4 pS/25 pS and the worst-case assumption of an equally favorable channel opening equilibrium constant [see Taylor and Baylor, 1995]), the probability that a given site is labeled would be 0.943, and the expected ratio of triply liganded to doubly-liganded channels would be 11. Finally, analysis below demonstrates that the assumption that covalent liganding is random can also be relaxed with little or no effect on the conclusions.

Evidence for Functional Heterogeneity in the cGMP-Binding Sites

On a simple basis, the dose–response relation for channels missing only a single ligand would be expected to follow a rectangular hyperbola (i.e., a Hill coefficient of 1.0) if all of the unliganded binding sites were identical. This is true for any single-site activation model, regardless of the number or nature of the conforma-

tional transitions (Fersht, 1985 [see also analysis in the next section]). Surprisingly, the concentration dependence of channel activation atop a fractional persistent current of 0.82 (Fig. 2) was much shallower than expected. In fact, the best fit of the Hill equation to the data was obtained with a coefficient of 0.65. The simplest model that can explain this behavior is one in which all of the channels are missing only a single ligand, but the individual binding sites fall into two classes with different apparent affinities. This type of model is described by the following equation:

$$I/I_{max} = F_1[cGMP]/([cGMP] + K_1) + F_2[cGMP]/([cGMP] + K_2), \quad (2)$$

where I/I_{max} is the fraction of maximum remaining current (atop the persistent current), F_1 and F_2 are the fractional abundances of the two classes of sites, and K_1 and K_2 are the apparent dissociation constants. The shallower dose–response behavior arises from different populations of sites because activation occurs over a wide range of cGMP concentrations. Fig. 3 compares the best fits of a single-site activation model and a two-site model to dose-response data atop a fractional persistent current of 0.77. Clearly, the single-site model is too steep to explain the data. On the other hand, a two-site model in which the sites exist in roughly equal proportions with apparent dissociation constants of 0.42 and 16 μM provides a good fit. Data consistent with these conclusions were obtained on 10 other patches from frog rods (seven) and salamander rods (three), in which Hill coefficients significantly less than one were obtained atop high levels of covalent activation (Table I). When dose–response relations atop comparable persistent currents were compared for all 11 patches (as in Fig. 2), the curves consistently superimposed.

A number of lines of evidence argue that the apparent binding-site heterogeneity reflects an intrinsic property of the channel, and is not an artifact introduced by the experimental conditions: (*a*) Currents achieved by complete covalent activation are the same as maximum cGMP-induced currents prior to covalent labeling (Brown et al., 1993*b*), and the conductances of single expressed homomultimeric channels activated in both ways are the same (M. L. Ruiz and J. W. Karpen, unpublished results). These results suggest that covalently attached ligands are as effective in promoting the conformational transition to an open state as reversibly-bound ligands; this transition affects apparent affinities, especially at the final binding site (Karpen et al., 1988*a*). The results also suggest that the process of covalent liganding does not cause any noncompetitive inhibition of channel function. (*b*) After permanent activation of some of the channels, the entire dose response relation for the remaining channels is shifted to lower concentrations, i.e., the relations do not cross

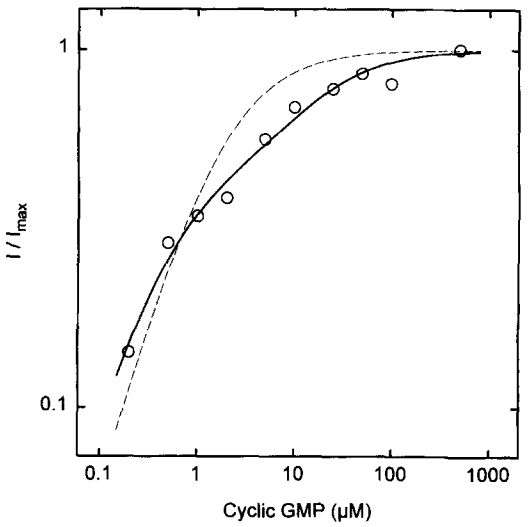

FIGURE 3. Functional heterogeneity in the cGMP-binding sites of the rod channel. Dose–response relation atop a persistent current that was 77% of the maximum cGMP-induced current. Data is from one of the patches shown in Fig. 2; measured currents were defined in the legend. The dashed curve is the best fit to the data of the following equation describing a single-site activation model: $I/I_{max} = [cGMP]/([cGMP] + K)$, where K is the apparent dissociation constant (1.6 μM). The solid curve is the best fit of Eq. 2 (see text) to the data with the following parameters: $F_1 = 0.44$, $K_1 = 0.42$ μM, $F_2 = 0.56$, and $K_2 = 16$ μM.

(see Fig. 2). If binding sites of lower apparent affinity like those described above were created by the experimental conditions, some channels would likely require a higher concentration of cGMP for activation than they did before exposure to APT-cGMP and UV light. (*c*) There is only a small left shift in the dose–response relation (Fig. 4) and a small degree of covalent activation observed (1–2%) when a high concentration of

TABLE I

Fits of the Hill Equation to cGMP Dose–Response Relations atop Different Levels of Covalent Activation (Native and Expressed Channels)

% Covalent activation	No. of Patches	n	$K_{1/2\text{-p}}/K_{1/2}$
0 (*N**)	11	2.1 ± 0.28	1.0
1.5 ± 0.41 (*N*)	3	1.4 ± 0.17	0.77 ± 0.021
21 ± 5.1 (*N*)	6	1.0 ± 0.12	0.37 ± 0.11
55 ± 6.4 (*N*)	6	0.80 ± 0.045	0.22 ± 0.052
76 ± 7.6 (*N*)	4	0.67 ± 0.046	0.20 ± 0.047
0 (*E*‡)	10	2.0 ± 0.35	1.0
76 ± 2.9 (*E*)	10	0.78 ± 0.12	0.52 ± 0.32

% Covalent activation is defined as $I_p/I_{max} \times 100$ (see Fig. 1 legend); n and $K_{1/2\text{-p}}/K_{1/2}$ (Hill equation parameters) were defined in the Fig. 2 legend. **N* represents native channels, and ‡*E* represents expressed channels (described earlier). Values are expressed as mean ± SD. For native channels, $K_{1/2}$ before covalent activation was 29 ± 9.3 μM (range 13–43 μM); for expressed channels, $K_{1/2}$ was 57 ± 25 μM (range 27–97 μM).

8-Br-cGMP is added to protect ligand-binding sites during a 4-min exposure to APT-cGMP and UV light. 8-Br-cGMP, like APT-cGMP, activates the channel at about a 10-fold lower concentration than cGMP (Zimmerman et al., 1985; Koch and Kaupp, 1985; Brown et al., 1993*b*). The magnitude of the left shift is comparable to that seen in other patches in which a similar degree of covalent activation was developed after only a 10–20-s exposure. This indicates that the long exposure time in this patch had no effects on the channel that cannot be explained by the level of covalent liganding. The slow onset of covalent activation in the presence of 8-Br-cGMP is yet another indication that persistent currents arise from labeling of the channel's cGMP binding sites. The effectiveness of 5 mM 8-Br-cGMP in preventing covalent activation is less than one might expect, based on the percentage of the time that it should occupy available binding sites. It has been observed in photoaffinity labeling, however, that competing ligands are not as effective in preventing covalent labeling as would be predicted by the dissociation constants of the two ligands (see e.g., Rogers and Parsons, 1992). The molecular basis for this phenomenon is not well understood, although it is thought to result from long-lived photolysis intermediates (Bayley, 1983). (*d*) As shown in the next section, models incorporating both apparent affinities provide a good fit to the original dose–response relation of a patch. A successful fit could not be obtained using only one of the apparent affinities, regardless of the assumptions made about channel-opening equilibria. This indicates that neither the high nor the low apparent affinity alone was created by the process of covalent activation. We cannot completely rule out the possibility that the sites are initially homogeneous, but because of a structural difference, label in such a way that the last open sites have different apparent affinities. Fortuitously, these affinities could appear to describe the original dose–response relation. If such a mechanism were true, however, the experiments would still be revealing a structural heterogeneity in the binding sites.

The conclusion that the ligand binding sites are heterogeneous does not depend on the initial assumption that the sites were labeled randomly. In fact, if covalent attachment at two different binding sites occurred with somewhat different efficiencies, a higher than expected proportion of channels would be missing a ligand at one class of site (the one that labels with lower efficiency), resulting in a measured Hill coefficient closer to 1.0.

Binding-Site Heterogeneity and Activation of the Rod cGMP-gated Channel

Fig. 5 illustrates three different mechanisms that might explain the functional heterogeneity in the final binding step. All three models assume that there are four

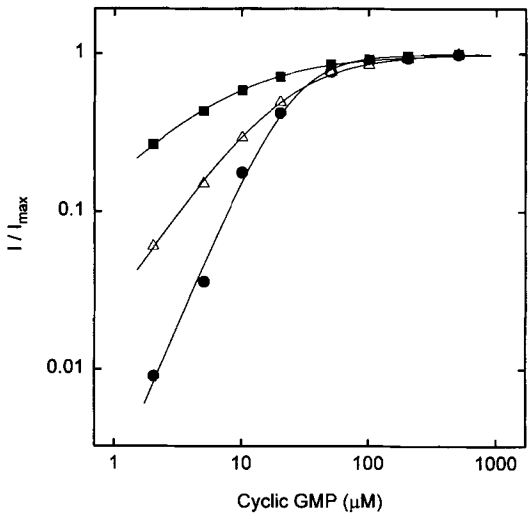

FIGURE 4. 8-Br-cGMP inhibits covalent activation of the rod channel. Dose–response curves for channels before exposure to APT-cGMP and UV light (*closed circles*), for channels that remained to be fully activated after a 4-min exposure to 10 μM APT-cGMP and UV light in the presence of 5 mM 8-Br-cGMP (*open triangles*), and for channels that remained to be fully activated after a subsequent 4-min exposure to 10 μM APT-cGMP and UV light (*closed squares*). The 4-min exposure in the presence of 8-Br-cGMP caused a persistent current that was 1–2% of the maximum cGMP-induced current of the patch (1,705 pA). The range given is due to a small uncertainty in the leak current (see Methods). The subsequent 4-min exposure in the absence of 8-Br-cGMP caused a persistent current that was 30% of the maximum cGMP-induced current. Smooth curves were fits of the Hill equation to the data with the following parameters: (*closed circles*) $n = 1.9$ and $K_{1/2} = 24$ μM; (*open triangles*) $n = 1.2$ and $K_{1/2} = 21$ μM; (*closed squares*) $n = 0.87$ and $K_{1/2} = 6.5$ μM.

cGMP-binding subunits, falling into two distinct classes; tethering of cGMP to three sites generates two channel populations having different apparent affinities for cGMP. In Model 1 (Fig. 5 *A*), this arises from binding sites that have different intrinsic affinities for cGMP. Model 2 (Fig. 5 *B*) is a variation on the first model, in which heterogeneity arises from different intrinsic affinities, but triply liganded channels can open to a partial or small conductance state. In Model 3 (Fig. 5 *C*), the different apparent affinities arise because one class of triply liganded channels opens to a subconducting state, while the other class does not. In this case, both subunit types have identical intrinsic affinities, but the channels undergo different opening transitions depending on which combination of subunits is occupied by cGMP. The apparent affinity at one site is lower because the open-closed transition to the subconducting state tends to stabilize the triply liganded form of the channel. In all of the models, fully liganded channels undergo a favorable transition to an open state.

To determine if the observed heterogeneity reflects an intrinsic property of the channel and to distinguish

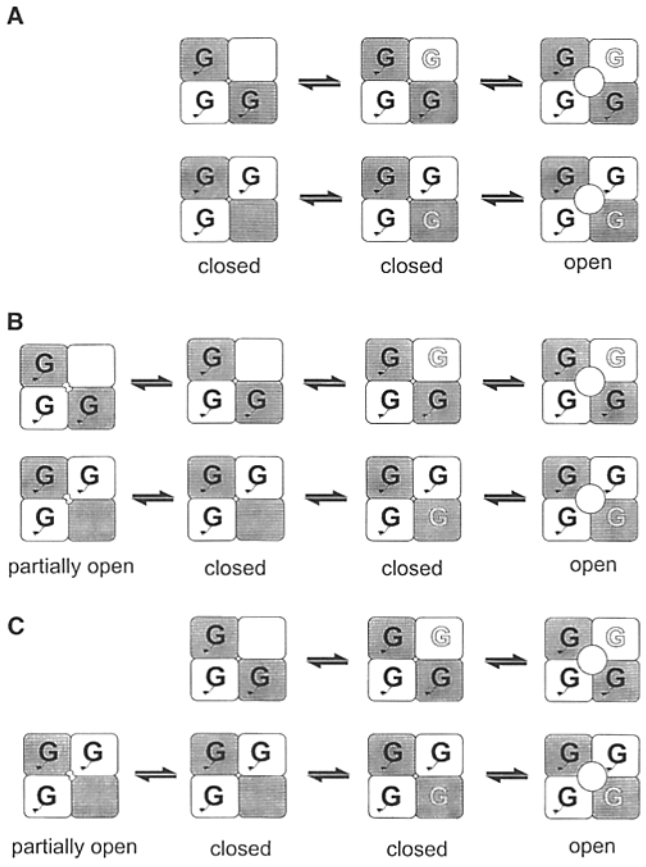

FIGURE 5. Models that might account for the observed heterogeneity in the final binding step. In each model there are four cGMP-binding sites, two of one type and two of another. cGMP moieties are covalently tethered to all but one site, leaving an equal mixture of the two types of sites unoccupied. Free cGMP can bind to the lone remaining site, and fully liganded channels can open to a large conductance state. (*A*) Model 1: heterogeneity arises from binding sites that have different intrinsic affinities for cGMP. (*B*) Model 2: heterogeneity arises from different intrinsic affinities as in Model 1, but all triply liganded channels can open to a partial or small conductance state. (*C*) Model 3: heterogeneity arises because half of the triply liganded channels open to a subconductance state, while the other half do not (depending on which combination of subunits is occupied). Both sites have identical intrinsic affinities.

between the models shown in Fig. 5, we attempted to fit a patch's original dose–response relation using the two apparent affinities revealed by the covalent activation method. Each model predicts two apparent dissociation constants in the last cGMP-binding step that have somewhat different dependencies upon both the intrinsic dissociation constants of binding and the equilibrium constants describing channel opening. In Model 1, in which the intrinsic binding affinities are different, the two apparent dissociation constants are given by the following equations:

$$K_1 = K_A K_L/(1 + K_L) \quad (3)$$

$$K_2 = K_B K_L/(1 + K_L), \quad (4)$$

where K_A and K_B are the intrinsic dissociation constants for binding and K_L is the channel closing equilibrium constant. For each fit to the original dose–response relation, a value of K_L was assumed, the corresponding values of K_A and K_B were calculated, and then values for I/I_{max} were calculated for the overall channel activation model (equations in Methods). This model has no additional free parameters; the early binding steps are described by K_A and K_B, and channel species with less than four ligands bound do not open. Using this simple model, a reasonable fit to the original dose–response relation was obtained only for values of K_L near 7.0 (Fig. 6 *A*). This value is much higher (indicating less favorable opening) than those reported in previous studies (Karpen et al., 1988; Matthews and Watanabe, 1988; Haynes and Yau, 1990; Taylor and Baylor, 1995); at positive membrane potentials, values ranging from 0.11 to 0.79 have been obtained (corresponding to open probabilities of 0.9 to 0.56). In a recent high-resolution study of single-channel patches from rod outer segments (Taylor and Baylor, 1995), the K_L value of 0.79 was reported. As shown in Fig. 6 *A*, this value predicts an original dose–response relation that is shifted to high concentrations with respect to the data. Lower K_L values predict dose-response relations that are shifted even farther to the right.

A good fit to the original dose-response relation, using realistic values of K_L, was obtained with Model 2 in Fig. 5 *B*. We retain the assumption that the observed heterogeneity arises solely from differences in the intrinsic binding affinities, but expand the first model to include a transition to a partially-conducting open state from either of the triply liganded channel species. This type of transition has no impact on the observed heterogeneity because it affects both triply-liganded species equally, but the presence of a subconductance state dictates higher intrinsic affinities at each site to explain the apparent affinities. The higher intrinsic affinities translate into an overall shift of the predicted dose–response relation to lower concentrations. In this model, the two apparent affinities are defined by the following equations:

$$K_1 = K_A K_L (1 + K_S)/[K_S (1 + K_L)] \quad (5)$$

$$K_2 = K_B K_L (1 + K_S)/[K_S (1 + K_L)], \quad (6)$$

where K_S is the channel closing equilibrium constant for the subconducting state, and the other constants were defined earlier. Assuming a K_L value of 0.79 (see above), a good fit to the original dose–response curve was obtained with a K_S value of 2.9 (Fig. 6 *B*). This value seems broadly consistent with measured behavior of

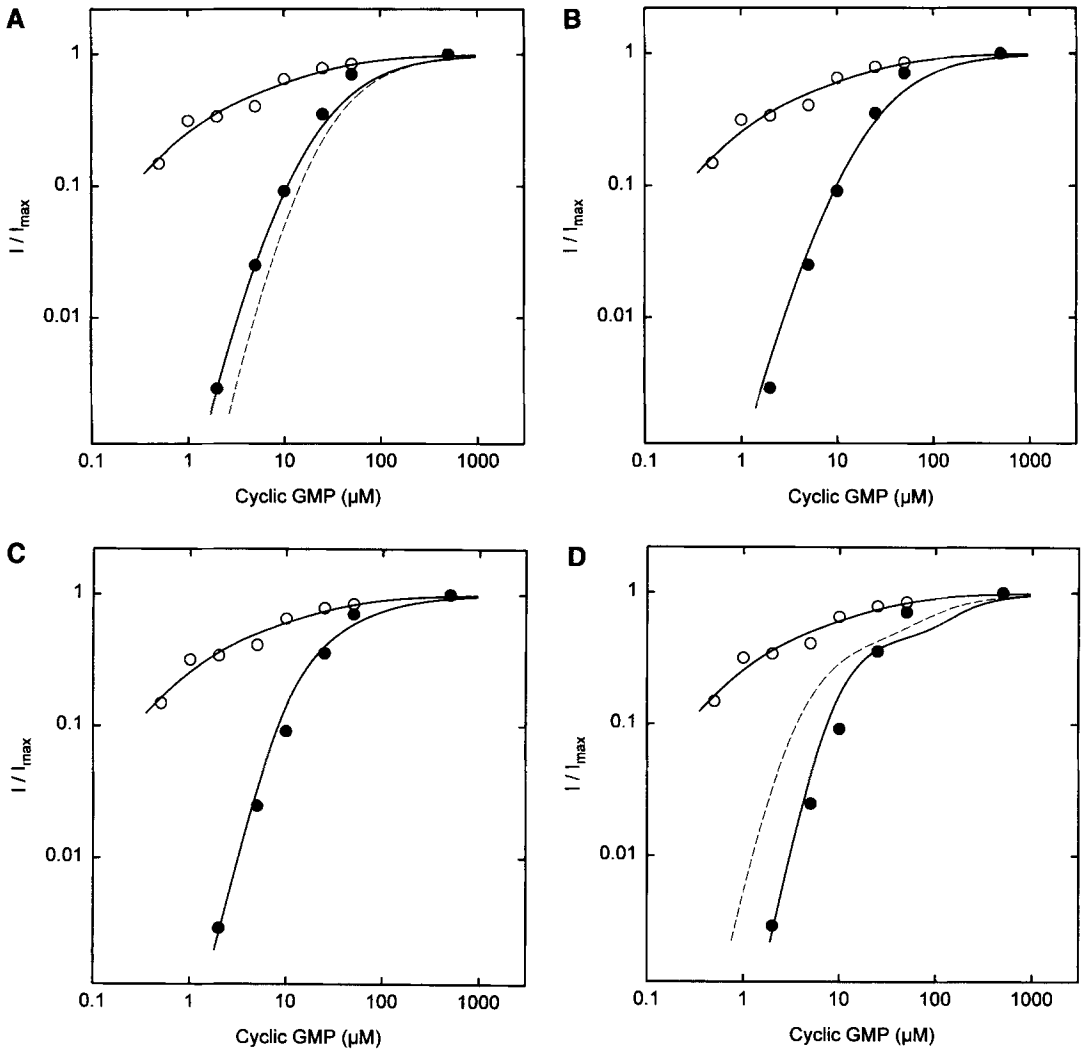

FIGURE 6. Fits of different channel models that incorporate heterogeneity in the last binding site to the original cGMP dose–response relation before covalent activation. Data is from one of the patches shown in Fig. 2; measured currents were defined in the legend. The filled circles represent the original dose–response relation and the open circles represent data atop a persistent current that was 87% of the maximum cGMP-induced current. In all four panels, the fit shown to the latter relation was obtained with Eq. 2 and the following parameters: $F_1 = 0.5$, $K_1 = 1.2$ μM, $F_2 = 0.5$, $K_2 = 19$ μM. These values of K_1 and K_2 were used to calculate the values of the intrinsic parameters for each mechanism (see text). (*A*) Original dose–response relation fit with Model 1, in which heterogeneity arises as shown in Fig. 5 *A*. (*Dashed curve*) K_L was assumed to be 0.79, K_A and K_B were calculated to be 2.8 and 42 μM (from Eqs. 3 and 4), and I/I_{max} values were calculated using equations for Model 1 (Methods). (*Solid curve*) K_L was assumed to be 7.0, and K_A and K_B were calculated to be 1.4 and 21 μM. There was little improvement in the fit when K_L values >7.0 were assumed. (*B*) Original dose–response relation fit with Model 2, in which heterogeneity arises as shown in Fig. 5 *B*. (*Smooth curve*) $K_L = 0.79$, $K_S = 2.9$, and the ratio of the open-channel conductance of the small state to that of the large state, r, was assumed to be 0.16 (Taylor and Baylor, 1995). K_A and K_B were calculated to be 2.1 and 31 μM (from Eqs. 5 and 6), and I/I_{max} values were calculated using equations for Model 2 (Methods). (*C*) Original dose–response relation fit with Model 3, in which heterogeneity arises as shown in Fig. 5 *C*. (*Smooth curve*) K_S was constrained to be 0.071 to account for the difference between K_1 and K_2 (Eqs. 7 and 8), $r = 0.16$, and $K_L = 0.055$. K_A was calculated to be 24 μM, and I/I_{max} values were calculated using equations for Model 3 (Methods). (*D*) Original dose–response relation fit with Model 4, in which heterogeneity arises because of two different types of channels that have different intrinsic affinities for cGMP. (*Dashed curve*) $K_L = 0.79$, K_A and K_B were calculated to be 2.8 and 42 μM (Eqs. 3 and 4), and I/I_{max} values were calculated using equations for Model 4 (Methods). (*Solid curve*) $K_L = 0.13$, and K_A and K_B were calculated to be 11 and 160 μM.

the small conductance state (Taylor and Baylor, 1995); a channel closing equilibrium constant was not determined, but opening to this state from partially-liganded channels was at least several times less favorable than opening to the large state from fully liganded channels.

In Model 3 (Fig. 5 *C*), in which the observed heterogeneity arises solely from differences in the ability of

triply liganded channels to open to a subconducting state, the apparent affinities are given by the following equations:

$$K_1 = K_A K_L / (1 + K_L) \quad (7)$$

$$K_2 = K_A K_L (1 + K_S) / [K_s (1 + K_L)], \quad (8)$$

where K_S is the channel closing equilibrium constant that describes the transition to a subconducting state from only one triply liganded channel species. The constants K_L and K_A have been defined and are identical for both species. To fully account for the observed difference between K_1 and K_2, the value of K_S is constrained to be 0.071. A fit to the original dose–response relation was obtained with a K_L value of 0.055 (Fig. 6 *C*). These opening transitions are unrealistically favorable (particularly the value of K_S), which suggests that the heterogeneity does not arise primarily from this type of behavior. This sort of mechanism, however, could be responsible for part of the observed heterogeneity.

The binding-site heterogeneity appears to be mainly an intrachannel rather than an interchannel phenomenon. We were unable to fit the original dose–response relation with the assumption that the two apparent affinities at the last binding step arose because of the existence of two different channel types. Regardless of the assumptions made about channel opening equilibria, such a mechanism predicted an obvious kink in the original relations (Fig. 6 *D*), which has never been observed.

The data presented here are not sufficient to rule out three- or five-site models of the channel, because we still lack detailed information about the early steps in the activation process. Assuming, however, that the intrinsic affinities at the two types of sites do not depend on the number of ligands bound, and that significant conformational transitions (to open states) occur only after the binding of the penultimate and ultimate ligands, it was more difficult to fit the original dose–response relation with three- or five-site models. For three-site models, the recently measured value of 0.79 for the channel closing equilibrium constant (Taylor and Baylor, 1995) predicts an original relation that is shifted slightly to the left of the data, and including a small conductance state from doubly liganded channels (the minimum model proposed in that study) predicts a curve that is shifted even farther to the left. For five-site models, a very favorable subconductance state arising from channels that contain four bound ligands was needed to fit the original dose–response relation (K_S = 1.2 and K_L = 0.79). The assumption made here, that significant conformational transitions occur only after the last two binding steps, is not in conflict with the recent proposal that activation of the homomultimer of the α subunit occurs when cGMP binds to the open state and progressively stabilizes that conformation (a Monod-Wyman-Changeux type allosteric model [Goulding et al., 1994]). In that study, the channel closing equilibrium constant was proposed to be 0.084 for a fully liganded channel and to increase by a factor of 33 for each ligand that unbinds, making opening quite unfavorable from channels missing more than one ligand.

As described earlier, dose–response data from other patches are virtually superimposable when cGMP concentrations are expressed relative to the concentration that gave a half-maximal current before covalent activation. Therefore, very similar conclusions are reached in fitting the models in Fig. 5 to data from different patches. Because the overall sensitivity to cGMP does vary (see Table I, legend), the absolute values of the fit parameters also vary. The relative heterogeneity in the binding sites, however, appears to be a robust property of all the patches examined.

Testing the Hypothesis that Binding Site Heterogeneity Arises from the Two Subunit Types

The discovery of functional heterogeneity among the cGMP-binding sites in the native channel raises the intriguing question of whether this behavior arises from two distinct subunits with different intrinsic properties, or from differential modulation of originally similar sites. Based on previous work, there are reasons to believe that both mechanisms may be operative. First, the sequence of the 240-kD β subunit shows only 50% identity with the α subunit in the cGMP-binding region (Chen et al., 1993; Körschen et al., 1995; Brown et al., 1995). These results make it seem likely that the β subunit would bind cGMP with a different affinity. Second, results from Gordon et al. (1992) indicate that endogenous mechanisms in the rod can modulate the channel's apparent affinity for cGMP. They reported spontaneous shifts of the dose–response relation over time after the excision of patches from amphibian rods. These shifts could be blocked by bath application of protein phosphatase inhibitors or accelerated by application of purified protein phosphatases, suggesting that phosphorylation plays a role in regulating the apparent affinity for cGMP.

To test the simple hypothesis that the heterogeneity observed in the native channel originated solely from the presence of two distinct subunits, homomultimeric versions of the channel composed of the bovine α subunit (Kaupp et al., 1989) were expressed in *Xenopus* oocytes, and tested for binding site heterogeneity after the covalent attachment of all but one ligand. The Hill coefficients of the dose–response relations were much more variable than in native rod channels (Fig. 7 and Table I), ranging from 0.62 to 0.97 in 10 patches. (The shift in $K_{1/2}$ after covalent activation was smaller and also much more variable than in native channels [Ta-

ble I].) The variability suggests that oocytes possess mechanisms capable of modifying the apparent affinity of the subunits for cGMP. In two patches, however, it is important to note that the data were fit with a Hill coefficient near unity, indicating that all of the subunits present in these channels behaved in a similar fashion. (In a third patch a value of 0.87 was obtained.) These results are significant for two reasons. First, the absence of heterogeneity in two patches provides further evidence that the heterogeneity seen in the native channels was not an artifact caused by the experimental manipulations. Second, Hill coefficients near 1.0 were never seen in native-channel patches. As described earlier, the Hill coefficient for native channels missing only a single ligand was invariably between 0.6 and 0.7, even on patches whose original $K_{1/2}$ values varied by a factor of three. The consistency of this result, found across patches in which some unknown form of channel regulation was changing, suggests that another factor is the dominant source of heterogeneity in native channels, perhaps the presence of two distinct subunit types. Further testing of this hypothesis may require the ability to control or eliminate regulatory mechanisms that can create heterogeneous behavior in expressed homomultimers, followed by coexpression studies using the β subunit.

In light of these results, it may seem curious that Chen et al. (1993) and Körschen et al. (1995) reported no difference in the dose–response relations between homomeric and heteromeric versions of the channel expressed in HEK-293 cells. At least two explanations for this are possible, however. (*a*) It seems likely that the properties of the α subunit assembled in a homomultimer would not be the same as those exhibited in a heteromultimer. For example, the concentration of cGMP that causes a half-maximal current ($K_{1/2}$) is a function of both binding and channel gating (see Goulding et al., 1994; Gordon and Zagotta, 1995), and coexpression of the β subunit has been shown to alter single-channel gating characteristics (Chen et al., 1993; Körschen et al., 1995). A subconductance state is apparent, and rapid flickering between closed and open states reminiscent of the native channel is restored. Thus, the observation of a similar $K_{1/2}$ upon coexpression of the β subunit does not rule out a significant functional heterogeneity in the behavior of the two subunit types. (*b*) There may be species differences in the degree of functional heterogeneity. The coexpression studies were done with cloned human (Chen et al., 1993) and bovine (Körschen et al., 1995) sequences.

For comparison, it is interesting to note that the native olfactory cyclic nucleotide-gated channel is activated by ~2.5-fold lower concentrations of cGMP than cAMP (Nakamura and Gold, 1987; Frings et al., 1992), while the homomultimer of the first subunit exhibits a

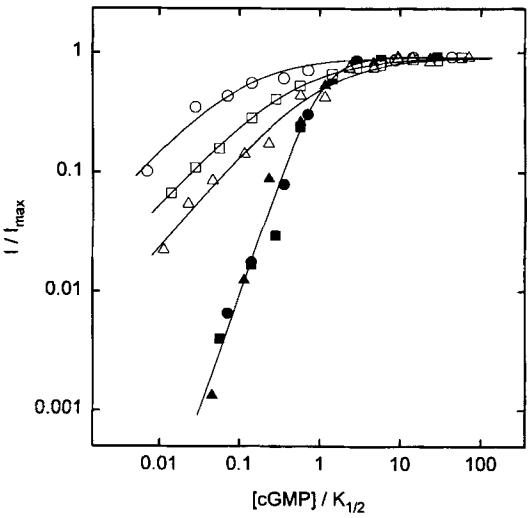

FIGURE 7. Evidence that the last binding site of expressed homomultimeric channels can either behave homogenously, or exhibit varying degrees of heterogeneity. Dose–response relations for channels in *Xenopus* oocytes consisting of the bovine α subunit, before covalent activation (*closed symbols*), and atop a high persistent current (≥75% of the maximum patch current [*open symbols*]). Measured currents were defined in the Fig. 2 legend. Data from three patches were normalized by expressing cGMP concentrations relative to the concentration that gave a half-maximal current before covalent activation ($K_{1/2}$). Each symbol shape is from a different patch. The original maximum currents and $K_{1/2}$ values for the three patches were: 7,580 pA and 44.4 μM (*triangles*); 10,850 pA and 36.2 μM (*squares*); 11,670 pA and 72 μM (*circles*). The smooth curves are fits to the modified form of the Hill equation given in legend to Fig. 2: (*closed symbols*) 0% persistent current, n = 2.0 and $K_{1/2\text{-p}}/K_{1/2}$ = 1.0; (*open triangles*) 75% persistent current, n = 0.96 and $K_{1/2\text{-p}}/K_{1/2}$ = 0.84 (linear fit parameters [see Methods]), n = 0.82 and $K_{1/2\text{-p}}/K_{1/2}$ = 0.91 (log fit parameters); (*open squares*) 82% persistent current, n = 0.76 and $K_{1/2\text{-p}}/K_{1/2}$ = 0.42; (*open circles*) 79% persistent current, n = 0.62 and $K_{1/2\text{-p}}/K_{1/2}$ = 0.092 (linear fit parameters), n = 0.79 and $K_{1/2\text{-p}}/K_{1/2}$ = 0.086 (log fit parameters).

30-fold preference for cGMP. Coexpression of the second subunit restores sensitivity to cAMP and reduces the apparent affinity for cGMP (Liman and Buck, 1994; Bradley et al., 1994).

The functional heterogeneity in the binding sites of the rod cGMP-gated channel, arising apparently from differences in the intrinsic affinities of the subunits for cGMP, is a previously unknown feature of channel function that will have to be taken into account as more is learned about the gating mechanism and the modulation of this type of channel. What purpose might two different types of cGMP binding sites serve? There is no definite answer at this time, but it seems attractive to suppose that the lower affinity site may have a faster off rate, allowing for more rapid channel closure in response to a light-induced decrease in the cGMP con-

centration. Although channel gating is much faster than the single photon response of a rod, it was pointed out previously that very rapid gating kinetics help the single photon response to stand out from channel noise in darkness (Karpen et al., 1988*b*). The higher affinity site, meanwhile, would give the overall channel a higher sensitivity to cGMP, so that lower cGMP concentrations would be required to achieve a certain level of dark current. Two different types of cGMP-binding sites may also allow for more flexible and graded modulation of channel function. Already there is evidence that the two types of subunits may be subject to different kinds of modulation. Transition metal divalent cations are known to potentiate the effect of cGMP on the channel, causing a shift in the dose–response relation to lower concentrations (Ildefonse and Bennett, 1991; Karpen et al., 1993); recent evidence suggests that they stabilize the open conformation of the channel, and bind to a histidine residue (H420) in the α subunit (Gordon and Zagotta, 1995). There is no corresponding histidine residue in the β subunit. On the other hand, the complex of Ca^{2+} and calmodulin has been shown to shift the dose–response to higher concentrations (Hsu and Molday, 1993; Gordon et al., 1995), and evidence suggests that the complex interacts with the β subunit (Hsu and Molday, 1993; Chen et al., 1994). The techniques described here should be useful for studying channel modulation at the level of the individual cGMP-binding sites. They should also be particularly useful at the single-channel level. In that setting, the covalent tethering of cGMP to the channel's binding sites will permit the isolation of channels with a fixed number of bound ligands. This promises to be a valuable tool to determine the origin of different conducting states, to learn more about the early steps in the activation process, and to dissect the contribution of individual subunits to overall channel function.

We thank Dr. William Zagotta for the bovine retinal cDNA clone. We also thank Drs. Denis Baylor, Yiannis Koutalos, and MariaLuisa Ruiz for comments on the manuscript.

This work was supported by a grant from the National Eye Institute (EY-09275 to J. W. Karpen). R. L. Brown was the recipient of a National Research Service Award (EY-06425).

Original version received 26 September 1995 and accepted version received 15 November 1995.

REFERENCES

Andersen, O. S., and R. E. Koeppe, II. 1992. Molecular determinants of channel function. *Physiol. Rev.* 72(Suppl.):S89–S158.

Barnard, E. A. 1992. Receptor classes and the transmitter-gated ion channels. *Trends Biochem. Sci.* 17:368–374.

Bayley, H. 1983. Photogenerated Reagents in Biochemistry and Molecular Biology. Elsevier Science Publishing Co., Inc., New York, NY.

Baylor, D. A., and B. J. Nunn. 1986. Electrical properties of the light-sensitive conductance of rods of the salamander *Ambystoma tigrinum*. *J. Physiol. (Lond.)*. 371:115–145.

Bradley, J., J. Li, N. Davidson, H. A. Lester, and K. Zinn. 1994. Heteromeric olfactory cyclic nucleotide-gated channels: a subunit that confers increased sensitivity to cAMP. *Proc. Natl. Acad. Sci. USA*. 91:8890–8894.

Brown, R. L., R. J. Bert, F. E. Evans, and J. W. Karpen. 1993*a*. Activation of retinal rod cGMP-gated channels: what makes for an effective 8-substituted derivative of cGMP? *Biochemistry*. 32:10089–10095.

Brown, R. L., W. V. Gerber, and J. W. Karpen. 1993*b*. Specific labeling and permanent activation of the retinal rod cGMP-activated channel by the photoaffinity analog 8-*p*-azidophenacylthio-cGMP. *Proc. Natl. Acad. Sci. USA*. 90:5369–5373.

Brown, R. L., R. Gramling, R. J. Bert, and J. W. Karpen. 1995. Cyclic GMP contact points within the 63-kDa subunit and a 240-kDa associated protein of retinal rod cGMP-activated channels. *Biochemistry*. 34:8365–8370.

Catterall, W. A. 1994. Molecular properties of a superfamily of plasma-membrane cation channels. *Curr. Opin. Cell Biol.* 6:607–615.

Chen, T.-Y., M. Illing, L. L. Molday, Y.-T. Hsu, K.-W. Yau, and R. S. Molday. 1994. Subunit 2 (or β) of retinal rod cGMP-gated cation channel is a component of the 240-kDa channel-associated protein and mediates Ca^{2+}-calmodulin modulation. *Proc. Natl. Acad. Sci. USA*. 91:11757–11761.

Chen, T.-Y., Y.-W. Peng, R. S. Dhallan, B. Ahamed, R. R. Reed, and K.-W. Yau. 1993. A new subunit of the cyclic nucleotide-gated cation channel in retinal rods. *Nature (Lond.)*. 362:764–767.

Fersht, A. 1985. Enzyme Structure and Mechanism. Second edition. W.H. Freeman and Company, New York, NY.

Fesenko, E. E., S. S. Kolesnikov, and A. L. Lyubarsky. 1985. Induction by cyclic GMP of cationic conductance in plasma membrane of retinal rod outer segment. *Nature (Lond.)*. 313:310–313.

Frings, S., J. W. Lynch, and B. Lindemann. 1992. Properties of cyclic nucleotide-gated channels mediating olfactory transduction. *J. Gen. Physiol.* 100:45–67.

Gordon, S. E., D. L. Brautigan, and A. L. Zimmerman. 1992. Protein phosphatases modulate the apparent agonist affinity of the light-regulated ion channel in retinal rods. *Neuron*. 9:739–748.

Gordon, S. E., J. Downing-Park, and A. L. Zimmerman. 1995. Modulation of the cGMP-gated ion channel in frog rods by calmodulin and an endogenous inhibitory factor. *J. Physiol. (Lond.)*. 486.3: 533–546.

Gordon, S. E., and W. N. Zagotta. 1995. A histidine residue associated with the gate of the cyclic nucleotide-activated channels in

rod photoreceptors. *Neuron.* 14:177–183.

Goulding, E. H., G. R. Tibbs, and S. A. Siegelbaum. 1994. Molecular mechanism of cyclic-nucleotide-gated channel activation. *Nature (Lond.).* 372:369–374.

Haynes, L. W., A. R. Kay, and K.-W. Yau. 1986. Single cyclic GMP-activated channel activity in excised patches of rod outer segment membrane. *Nature (Lond.).* 321:66–70.

Haynes, L. W., and K.-W. Yau. 1990. Single-channel measurement from the cyclic GMP-activated conductance of catfish retinal cones. *J. Physiol. (Lond.)* 429:451–481.

Hsu, Y.-T., and R. S. Molday. 1993. Modulation of the cGMP-gated channel of rod photoreceptor cells by calmodulin. *Nature (Lond.).* 361:76–79.

Ildefonse, M., and N. Bennett. 1991. Single-channel study of the cGMP-dependent conductance of retinal rods from incorporation of native vesicles into planar lipid bilayers. *J. Membr. Biol.* 123:133–147.

Karpen, J. W., R. L. Brown, L. Stryer, and D. A. Baylor. 1993. Interactions between divalent cations and the gating machinery of cyclic GMP-activated channels in salamander retinal rods. *J. Gen. Physiol.* 101:1–25.

Karpen, J. W., A. L. Zimmerman, L. Stryer, and D. A. Baylor. 1988*a*. Gating kinetics of the cyclic-GMP-activated channel of retinal rods: flash photolysis and voltage-jump studies. *Proc. Natl. Acad. Sci. USA.* 85:1287–1291.

Karpen, J. W., A. L. Zimmerman, L. Stryer, and D. A. Baylor. 1988*b*. Molecular mechanics of the cyclic-GMP-activated channel of retinal rods. *Cold Spring Harbor Symp. Quant. Biol.* 53:325–332.

Kaupp, U. B. 1991. The cyclic nucleotide-gated channels of vertebrate photoreceptors and olfactory epithelium. *Trends Neurosci.* 14:150–157.

Kaupp, U. B. 1995. Family of cyclic nucleotide gated ion channels. *Curr. Opin. Neurobiol.* 5:434–442.

Kaupp, U. B., T. Niidome, T. Tanabe, S. Terada, W. Bönigk, W. Stühmer, N. J. Cook, K. Kangawa, H. Matsuo, T. Hirose, T. Miyata, and S. Numa. 1989. Primary structure and functional expression from complementary DNA of the rod photoreceptor cyclic GMP-gated channel. *Nature (Lond.).* 342:762–766.

Koch, K.-W., and U. B. Kaupp. 1985. Cyclic GMP directly regulates a cation conductance in membranes of bovine rods by a cooperative mechanism. *J. Biol. Chem.* 260:6788–6800.

Körschen, H. G., M. Illing, R. Seifert, F. Sesti, A. Williams, S. Gotzes, C. Colville, F. Müller, A. Dosé, M. Godde, L. Molday, U.B. Kaupp, and R. S. Molday. 1995. A 240 kDa protein represents the complete β subunit of the cyclic nucleotide-gated channel from rod photoreceptor. *Neuron.* 15:627–636.

Liman, E. R., and L. B. Buck. 1994. A second subunit of the olfactory cyclic nucleotide-gated channel confers high sensitivity to cAMP. *Neuron.* 13:611–621.

Matthews, G., and S.-I. Watanabe. 1988. Activation of single ion channels from toad retinal rod inner segments by cyclic GMP: concentration dependence. *J. Physiol. (Lond.).* 403:389–405.

Nakamura, T., and G. H. Gold. 1987. A cyclic nucleotide-gated conductance in olfactory receptor cilia. *Nature (Lond.).* 325:442–444.

Pugh, E. N., Jr., and T. D. Lamb. 1993. Amplification and kinetics of the activation steps in phototransduction. *Biochim. Biophys. Acta.* 1141:111–149.

Rogers, G. A., and S. M. Parsons. 1992. Photoaffinity labeling of the acetylcholine transporter. *Biochemistry.* 31: 5770–5777.

Stryer, L. 1991. Visual excitation and recovery. *J. Biol. Chem.* 266: 10711–10714.

Taylor, W. R., and D. A. Baylor. 1995. Conductance and kinetics of single cGMP-activated channels in salamander rod outer segments. *J. Physiol. (Lond.).* 483.3:567–582.

Unwin, N. 1993. Neurotransmitter action: opening of ligand-gated ion channels. *Cell.* 72:*Neuron.*10:(Suppl.):31–41.

Yarfitz, S., and J. B. Hurley. 1994. Transduction mechanisms of vertebrate and invertebrate photoreceptors. *J. Biol. Chem.* 269: 14329–14332.

Yau, K.-W. 1994. Cyclic nucleotide-gated channels: an expanding new family of ion channels. *Proc. Natl. Acad. Sci. USA.* 91:3481–3483.

Yau, K.-W., and D. A. Baylor. 1989. Cyclic GMP-activated conductance of retinal photoreceptor cells. *Annu. Rev. Neurosci.* 12:289–327.

Zagotta, W. N., T. Hoshi, and R. W. Aldrich. 1989. Gating of single *Shaker* potassium channels in *Drosophila* muscle and in *Xenopus* oocytes injected with *Shaker* mRNA. *Proc. Natl. Acad. Sci. USA.* 86: 7243–7247.

Zimmerman, A. L. 1995. Cyclic nucleotide gated channels. *Curr. Opin. Neurobiol.* 5:296–303.

Zimmerman, A. L., and D. A. Baylor. 1986. Cyclic GMP-sensitive conductance of retinal rods consists of aqueous pores. *Nature (Lond.).* 321:70–72.

Zimmerman, A. L., J. W. Karpen, and D. A. Baylor. 1988. Hindered diffusion in excised membrane patches from retinal rod outer segments. *Biophys. J.* 54:351–355.

Zimmerman, A. L., G. Yamanaka, F. Eckstein, D. A. Baylor, and L. Stryer. 1985. Interaction of hydrolysis-resistant analogs of cyclic GMP with the phosphodiesterase and light-sensitive channel of retinal rod outer segments. *Proc. Natl. Acad. Sci. USA.* 82:8813–8817.